

^{233}U Cross-Section and Covariance Data Update for SCALE 5.1 Libraries

February 2008

Prepared by
L. C. Leal
D. Wiarda
B. T. Rearden
H. Derrien

DOCUMENT AVAILABILITY

Reports produced after January 1, 1996, are generally available free via the U.S. Department of Energy (DOE) Information Bridge.

Web site <http://www.osti.gov/bridge>

Reports produced before January 1, 1996, may be purchased by members of the public from the following source.

National Technical Information Service
5285 Port Royal Road
Springfield, VA 22161
Telephone 703-605-6000 (1-800-553-6847)
TDD 703-487-4639
Fax 703-605-6900
E-mail info@ntis.gov
Web site <http://www.ntis.gov/support/ordernowabout.htm>

Reports are available to DOE employees, DOE contractors, Energy Technology Data Exchange (ETDE) representatives, and International Nuclear Information System (INIS) representatives from the following source.

Office of Scientific and Technical Information
P.O. Box 62
Oak Ridge, TN 37831
Telephone 865-576-8401
Fax 865-576-5728
E-mail reports@osti.gov
Web site <http://www.osti.gov/contact.html>

This report was prepared as an account of work sponsored by an agency of the United States Government. Neither the United States Government nor any agency thereof, nor any of their employees, makes any warranty, express or implied, or assumes any legal liability or responsibility for the accuracy, completeness, or usefulness of any information, apparatus, product, or process disclosed, or represents that its use would not infringe privately owned rights. Reference herein to any specific commercial product, process, or service by trade name, trademark, manufacturer, or otherwise, does not necessarily constitute or imply its endorsement, recommendation, or favoring by the United States Government or any agency thereof. The views and opinions of authors expressed herein do not necessarily state or reflect those of the United States Government or any agency thereof.

Nuclear Science and Technology Division

**^{233}U CROSS-SECTION AND COVARIANCE DATA
UPDATE FOR SCALE 5.1 LIBRARIES**

L. C. Leal
D. Wiarda
B. T. Rearden
and
H. Derrien

Date Published: February 2008

Prepared by
OAK RIDGE NATIONAL LABORATORY
Oak Ridge, Tennessee 37831-6283
managed by
UT-BATTELLE, LLC
for the
U.S. DEPARTMENT OF ENERGY
under contract DE-AC05-00PR22725

CONTENTS

	<u>Page</u>
LIST OF FIGURES	v
LIST OF TABLES	vii
ACRONYMS	ix
ACKNOWLEDGMENTS	xi
ABSTRACT	xiii
1. INTRODUCTION	1
2. RESOLVED RESONANCE COVARIANCE EVALUATION	1
3. UNRESOLVED RESONANCE COVARIANCE EVALUATION.....	5
4. PROCESSING OF THE ²³³ U COVARIANCE DATA	7
5. PROCESSING OF ²³³ U ENDF FILE	11
6. BENCHMARK CALCULATIONS AND DATA UNCERTAINTY	17
7. CONCLUSIONS.....	29
8. REFERENCES	31

LIST OF FIGURES

<u>Figure</u>	<u>Page</u>
1. Comparison of average cross sections calculated with SAMMY with the experimental data.....	6
2. Total $\bar{\nu}$ and uncertainties calculated in the 44-neutron groups of the SCALE system.	8
3. Prompt $\bar{\nu}$ and uncertainties calculated in the 44-neutron groups of the SCALE system.	9
4. ^{233}U total cross section calculated in the 44-neutron group structure of the SCALE system.	10
5. ^{233}U fission cross section calculated in the 44-neutron group structure of the SCALE system.	10
6. ^{233}U capture cross section calculated in the 44-neutron group structure of the SCALE system.	11
7. Absolute k_{eff} uncertainties due to covariance data as a function of experiment number.	21
8. Absolute k_{eff} uncertainties due to covariance data as a function of EALF.	21
9. Absolute k_{eff} uncertainties due to covariance data for ^{233}U fission.....	22
10. Absolute k_{eff} uncertainties due to covariance data for ^{233}U $\bar{\nu}$	22
11. Absolute k_{eff} uncertainties due to covariance data for ^{233}U n,gamma.	23
12. Absolute k_{eff} uncertainties due to covariance data for ^{233}U elastic.	23
13. Absolute k_{eff} uncertainties due to covariance data for ^{233}U chi.	24
14. Absolute k_{eff} uncertainties due to covariance data for ^{233}U fission to ^{233}U elastic.	24
15. Absolute k_{eff} uncertainties due to covariance data for ^{233}U fission to ^{233}U n,gamma.	25
16. Absolute k_{eff} uncertainties due to covariance data for ^{233}U n,gamma to ^{233}U elastic.	25
17. Absolute k_{eff} uncertainties due to covariance data for ^{238}U fission to ^{233}U fission.	26
18. Absolute k_{eff} uncertainties due to covariance data for ^{235}U fission to ^{233}U fission.	26
19. Absolute k_{eff} uncertainties due to covariance data for ^{233}U n,2n.	27
20. Absolute k_{eff} uncertainties due to covariance data for ^{233}U n,n'.	27

LIST OF TABLES

<u>Table</u>	<u>Page</u>
1. Selected measurements for ^{233}U evaluation of RRR.....	3
2. Evaluated integral quantities.....	4
3. Uncertainty in the average fission and capture cross section calculated with PUFF-IV code using the RPCM	4
4. Average values of the resonance parameters input used in the SAMMY unresolved resonance calculations for orbital angular momentum $l = 0$	5
5. Average values of the resonance parameters and uncertainties calculated with the covariance data generated with SAMMY for orbital angular momentum $l = 0$	7
6. Uncertainty in the average fission and capture cross section calculated with PUFF-IV in the unresolved energy region.....	7
7. Benchmark experiments selected for verification of the ^{233}U covariance data	18

ACRONYMS

EALF	Energy of Average Lethargy Causing Fission
ENDF	Evaluated Nuclear Data Library
IAEA	International Atomic Energy Agency
ORELA	Oak Ridge Electron Linear Accelerator
ORNL	Oak Ridge National Laboratory
rel. s. d.	relative standard deviation
RPCM	Resonance Parameter Covariance Matrix

ACKNOWLEDGMENTS

The authors acknowledge two offices of the U.S. Department of Energy for sponsoring this work. These are DOE/NA-171 (Nuclear Criticality Safety Program) and DOE/EM-60 (EM Safety Management and Operations). Also it is acknowledged that K. R. Elam, formerly of the Oak Ridge National Laboratory performed the TSUNAMI calculations for this work.

ABSTRACT

Resonance parameter covariance data have been generated for ^{233}U in the resolved and unresolved resonance region using the computer code SAMMY. High-energy covariance uncertainties were generated at the International Atomic Energy Agency using the computer code EMPIRE. The covariance data were added to the ENDF/B-VII.0 evaluation of the ^{233}U cross sections. The covariance data were processed with the PUFF module in AMPX. Eighty-two benchmark calculations for systems including ^{233}U were done with the TSUNAMI sensitivity analysis sequence of the SCALE system. The work is in support of criticality safety evaluation of future operations at the Oak Ridge National Laboratory Building 3019.

1. INTRODUCTION

Resonance-parameter covariance matrix (RPCM) evaluation in the resolved and unresolved resonance regions were done for ^{233}U using the computer code SAMMY.¹ The RPCMs were obtained as a result of the resolved² and unresolved³ resonance regions evaluation. The evaluations were done separately; that is, the resolved resonance evaluation was performed from 0 to 600 eV, and the unresolved evaluation was performed from 600 eV to 40 keV.

In the resonance region, pointwise cross sections are reconstructed using the R-matrix cross-section formalism with evaluated resonance parameters. Uncertainties in the reconstructed cross section are obtained by propagating the uncertainties from the resonance parameters. For reactor applications, group cross sections are produced by weighting the pointwise cross sections with a neutron flux spectrum and integrating over energies within a group. Consequently, uncertainties in the group cross sections are also derived from uncertainties in the resonance parameters.

To understand how uncertainties in the resonance parameters are calculated, we must consider the process by which the parameters are determined: resonance parameters are obtained by fitting experimental data using generalized least-squares techniques in conjunction with R-matrix theory. In SAMMY, both systematic and statistical uncertainties in the experimental data are incorporated directly into the fitting procedure, which then determines the long-range correlations in the RPCM. The experimental uncertainties come from a variety of sources, such as normalization, background, neutron time-of-flight (TOF), and sample thickness. It is important that the evaluator understand and include the uncertainties associated with the experimental data to assess the impact of these uncertainties in the evaluation process.

High-energy covariance evaluation was performed at the International Atomic Energy Agency (IAEA) by Roberto Capote⁴ in coordination with Andrej Trkov and Mihaela Sin using the computer code EMPIRE.⁵ Estimation was based on a Monte Carlo sampling of the model parameters,⁵ taking such uncertainty of these parameters as to approximately cover the spread of the experimental data. Average uncertainties and the correlation matrices have been obtained following Donald Smith's formulation.⁶ A more rigorous approach would utilize the Generalized Least Squares method, in which the calculated model covariance is taken as a prior for the least squares fitting based on the GANDR system.⁷ However such an approach would require additional time and support. In addition to the RPCM and high-energy cross section uncertainty evaluations, covariance evaluation of the ^{233}U average number of neutrons released per fission was also performed.⁸ The approach used to evaluate the resonance covariance for ^{233}U will be presented here. The resulting covariance evaluations were converted into the ENDF format and processed with the computer codes PUFF-IV⁹ and ERRORJ.¹⁰

2. RESOLVED RESONANCE COVARIANCE EVALUATION

A Reich-Moore resolved resonance evaluation for ^{233}U was carried out with the code SAMMY in the energy region from 0 to 600 eV.² A total of 769 resonances, including the external levels,

was used. Each resonance of ^{233}U in the Reich-Moore formalism is described by five parameters (i.e., the resonance energy E_r , the gamma width Γ_γ , the neutron width Γ_n , and the two fission widths Γ_{f1} , and Γ_{f2}), for a total of 3845 parameters. The large number of resonance parameters leads to two major issues when generating a resonance covariance: (1) the large computer memory required to process the data and (2) the data storage for the resulting covariance file. The former has been addressed by using a DEC Alpha workstation with 32 GB of memory. The latter issue was not of a concern because the resulting ^{233}U covariance matrix in the ENDF format¹¹ is a manageable file of 100 MB.¹²

Several experimental data were used in the ^{233}U evaluation. To enable a SAMMY analysis of the ^{233}U cross sections at energies above 150 eV, two high-resolution measurements were performed at the Oak Ridge Electron Linear Accelerator (ORELA). Neutron transmission measurements with samples cooled to 11 K to reduce the Doppler effect, at a flight path of 79.8 m, were done by Guber et al.¹³ The transmission measurements done with the sample cooled to 11 K have led to a reduction of the width of the resonances by a factor of 2 compared to the experiments at room temperature. Two sets of measurements were done with different sample thicknesses: (1) a set of measurements with a sample of 0.00298 at/b in the energy region 0.5 to 80 eV and (2) a set of measurements of 0.0119 at/b in the energy range 6 eV to 300 keV. In addition to the transmission measurements, two sets of fission cross-section measurements at a flight path of 80 m were also carried out by Guber et al.¹⁴ in the energy ranges of 0.5 to 80 eV with a cadmium filter and another in the energy range from 10 eV to 700 keV with a ^{10}B filter, respectively. The fission cross-section measurements at the 80-m flight path have much better resolution than any of the previous fission measurements. These ORELA transmission and fission measurements were the primary data used in the ^{233}U evaluation in the energy range from 0.5 to 600 eV. Twelve measurements were included in the evaluation as shown in Table 1. Four of these measurements are the Oak Ridge National Laboratory (ORNL) transmission and fission cross section done by Guber et al. as explained above. The transmission measurements were done by Harvey et al.¹⁵ in 1979, transmission measurements done by Moore et al.¹⁶ in 1960, and transmission measurements done by Pattenden and Harvey¹⁷ in 1963. Two sets of simultaneous measurements of capture and fission data were performed by Weston et al.¹⁸ in 1970. Fission cross-section measurements were performed by Blons¹⁹ in 1973, and fission measurements were performed by Deruytter and Wagemans²⁰ in 1974.

In addition to the microscopic data (from TOF measurements), a variety of integral quantities are available within SAMMY. These integral quantities are calculated by integrating over the microscopic absorption, fission, and capture cross sections. The integral quantities used in the ^{233}U evaluation are the Westcott factor, the K_1 value, the resonance integral I_x , and the capture-to-fission ratio (the α -ratio). These quantities are defined as follows:

1. Westcott factor:

$$g_w = \frac{2}{\sqrt{\pi}} \frac{\sigma_x}{\sigma_{0x}},$$

where σ_x and σ_{0x} are the Maxwellian-averaged cross sections and the cross sections at 0.0253 eV.

2. K_1 factor:

$$K_1 = \nu \sigma_{0f} g_f - \sigma_{0a} g_a .$$

3. Resonance integral:

$$I_x = \int_{0.5eV}^{20MeV} \frac{\sigma_x}{E} dE .$$

4. α Ratio:

$$\alpha = \frac{I_c}{I_f} .$$

Some of the evaluated integral values for ^{233}U are shown in Table 2.

Table 1. Selected measurements for ^{233}U evaluation of RRR

Author	Energy region analyzed (eV)	Main features
Moore et al., 1960	0.020 – 15.0	Transmission; chopper, TOF 15.7-m sample 0.0037 and 0.0213 at/b
Pattenden and Harvey, 1963	0.080 – 15.0	Transmission; chopper, TOF 45-m sample 0.00057, 0.00308, 0.01219 at/b
Weston et al., 1968	1.0 – 600.0	Simultaneous measurements of capture and fission, Linac TOF 25.2 m
Weston et al., 1968	0.020 – 1.0	Simultaneous measurements of capture and fission, Linac TOF 25.6 m
Blons, 1973	4.0 – 600.0	Fission, Linac, TOF 50.1 m, sample at liquid nitrogen temperature
Deruyter and Wagemans, 1974	0.020 – 15.0	Fission, Linac, TOF 8.1 m
Harvey et al., 1979	0.020 – 1.2	Transmission, Linac, TOF 17.9-m sample 0.00605 and 0.0031 at/b
Wagemans et al., 1988	0.002 – 1.0	Fission, Linac, TOF 8.1 m
Guber et al., 1998	1.0 – 80.0	Transmission, Linac, TOF 80 m Cd filter, sample temperature 11 K Sample thickness 0.00298 at/b
Guber et al., 1998	7.0 – 600.0	Transmission, Linac, TOF 80 m ^{10}B filter, sample temperature 11 K Sample thickness 0.0119 at/b
Guber et al., 1998	1.0 – 80.0	Fission, Linac, TOF 80 m Cd filter
Guber et al., 1998	7.0 – 600.0	Fission, Linac, TOF 80 m ^{10}B filter

Table 2. Evaluated integral quantities

Quantity	ENDF/B-VI standard	Axton standard	BNL	Present work
g_a	0.9996 ± 0.0011	0.9995 ± 0.0011	0.9996 ± 0.0015	1.0003 ± 0.0009
g_f	0.9955 ± 0.0014	0.9955 ± 0.0014	0.9955 ± 0.0011	1.0004 ± 0.0012
I_a			897 ± 20	917.45 ± 8.0
I_f			760 ± 17	777.82 ± 5.0
K_1	742.60 ± 2.40	742.25 ± 2.37		746.77 ± 1.98

In the resonance parameter evaluation performed with SAMMY, the various cross sections were fitted using the R-matrix theory with the Reich-Moore approximation, including corrections for experimental conditions such as Doppler and resolution broadening, multiple scattering corrections, and backgrounds. The best fit to the experimental data is determined by means of a generalized least-squares fitting procedure. Experimental uncertainties are incorporated directly into the evaluation process to propagate those uncertainties into the resonance parameter results. Uncertainties treated in the evaluation process included statistical and systematic uncertainties for each different data set plus the quoted uncertainties for the integral data and thermal cross sections. The result of the evaluation is a complete RPCM associated with the resonance parameters. Average fission and capture cross sections and uncertainties calculated with the PUFF-IV code for a constant flux in energy intervals of 50 eV are shown in Table 3. The percentage cross section uncertainties relative standard deviation (rel. s. d.) are also shown. One can see that the average fission cross section uncertainties are from 0.9 to 2.2%, whereas the uncertainties for the average capture cross section are in between 2.4 to 3.7%.

Table 3. Uncertainty in the average fission and capture cross section calculated with PUFF-IV code using the RPCM

E_{\min} (eV)	E_{\max} (eV)	σ_f (barns)	Relative standard deviation (%)	σ_γ (barns)	Relative standard deviation (%)
10-5	50.0	84.905	0.9	13.857	2.4
50.0	100.0	39.053	1.0	7.313	2.6
100.0	150.0	29.719	1.0	4.876	2.7
150.0	200.0	20.973	1.1	3.062	2.7
200.0	250.0	23.080	1.1	3.758	2.8
250.0	300.0	23.139	1.1	3.263	2.9
300.0	350.0	17.400	1.3	2.369	2.8
350.0	400.0	19.148	1.3	2.525	3.1
400.0	450.0	9.712	1.8	1.143	3.9
450.0	500.0	12.395	1.7	1.623	3.1
500.0	550.0	14.604	1.8	1.781	3.2
550.0	600.0	12.433	2.2	2.228	3.7

3. UNRESOLVED RESONANCE COVARIANCE EVALUATION

An unresolved resonance evaluation for ^{233}U was done in the energy region from 600 eV to 40 keV. Above 600 eV the fluctuations in the measured cross sections are smaller than those in the resolved range but are still important for calculating the energy self-shielding of the cross section. These fluctuations are due to unresolved multiplets of resonances for which it is not possible to determine parameters of the individual resonances as is done in the resolved region. The mechanism utilized for the cross section treatment in the unresolved region is based on average values of physical quantities obtained in the resolved range. Knowledge of the average values for level spacings, strength functions, widths, and other relevant parameters is used to infer their behavior in the unresolved energy region.

Four sets of experimental data were used in the evaluation:

1. Effective average total cross sections of Guber et al.¹³ obtained from experimental transmission measurements. These transmission measurements were performed at a 79.8-m flight path with sample thicknesses of 0.0119 at/b and with the sample cooled to 11 K. The average cross sections were derived by Derrien et al.²¹ and corrected for self-shielding; the data were used from 600 eV to 40 keV.
2. Fission cross sections of Guber et al.¹⁴ taken on the 80-m flight path. These data were used from 600 eV to 40 keV.
3. Fission and capture data of Weston et al.¹⁸ obtained from the capture-to-fission ratio measurements done at a 25.2-m flight path from 600 eV to 2 keV.
4. Capture data of Hopkins extracted from capture-to-fission ratio measurements done with a collimated neutron beam incident in a target placed in a cadmium-loaded liquid scintillator.²²

The computer code SAMMY was used to fit the data in the energy region from 600 eV to 40 keV. The average parameters obtained in the resolved resonance region and used in the SAMMY unresolved fit are shown in Table 4. The parameters are total angular momentum J , average level spacing $\langle D \rangle$, strength function S_n , fission width $\langle \Gamma_f \rangle$, effective fission degrees of freedom N_{eff} , and capture width $\langle \Gamma_\gamma \rangle$.

Table 4. Average values of the resonance parameters input used in the SAMMY unresolved resonance calculations for orbital angular momentum $l=0$

J	$\langle D \rangle$ (eV)	$S_n \times 10^4$	$\langle \Gamma_f \rangle$ (meV)	N_{eff}	$\langle \Gamma_\gamma \rangle$ (meV)
Mixed levels	0.52 ± 0.08	0.895 ± 0.047	496		39.0 ± 3.0
2+	1.19 ± 0.12		760 ± 60	4.0	
3+	0.92 ± 0.10		296 ± 30	2.0	

The resulting unresolved parameters obtained from the SAMMY fit were reported to ENDF at 29 reference energies. The reference energies were determined based on the observed fluctuations

in the experimental data, which result from unresolved multiplets of resonances. These reference energies are 600, 682.5, 765, 872.5, 990, 1125, 1250, 1340, 1410, 1470, 1585, 1735, 1880, 2107.5, 2522.5, 3120, 447.5, 6250, 7275, 7775, 8350, 9350, 11000, 13500, 17500, 22500, 27500, 32500, and 40000 eV.

The results of the fit of the experimental data are given in Fig. 1. The experimental cross-section data shown in Fig. 1 are the total cross section of Guber et al.,¹³ the fission cross section of Guber et al.,¹⁴ the capture cross section of Weston et al.,¹⁸ and the capture cross section of Hopkins et al.²² The solid line represents the SAMMY fit to the data showing good agreement with the experimental data.

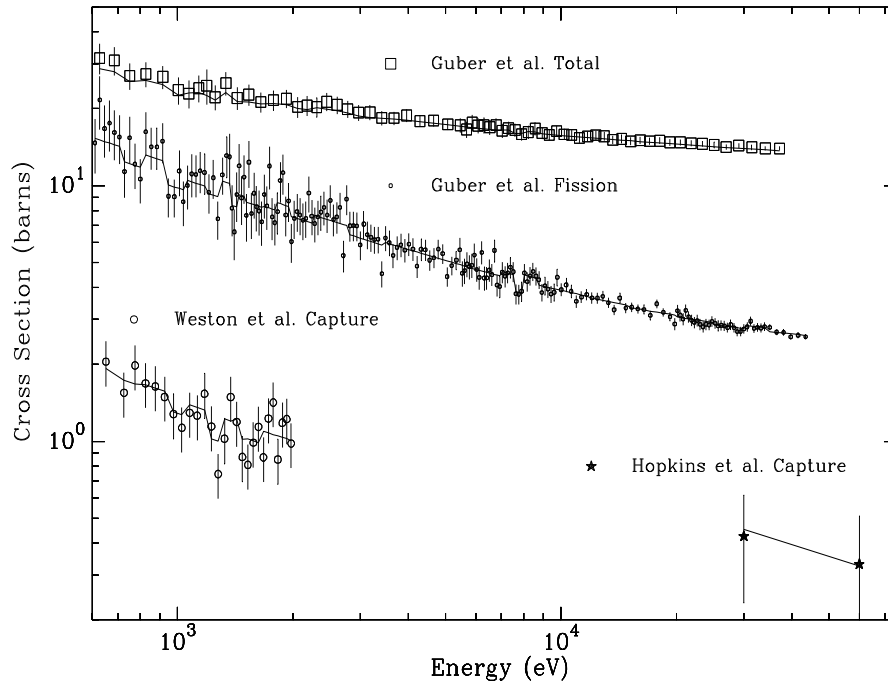


Fig. 1. Comparison of average cross sections calculated with SAMMY with the experimental data.

The RPCM matrix associated with the unresolved resonance parameters was obtained with SAMMY by fitting the experimental data, including the statistical and systematic uncertainties of the experimental data. Note that the data normalization is the most important issue in determining the average parameter covariance data. Because of limitation in the ENDF format, covariance data for the average resonance parameters can only be provided for the entire energy region, that is, from 600 eV to 40 keV. The uncertainties for average s -wave ($l = 0$) resonance parameters calculated with the covariance data are given in Table 5.

Table 5. Average values of the resonance parameters and uncertainties calculated with the covariance data generated with SAMMY for orbital angular momentum $l=0$

J	$S_n \times 10^4$	$\langle \Gamma_f \rangle$ (meV)	$\langle \Gamma_\gamma \rangle$ (meV)
Mixed levels	0.939 ± 0.036	496	39.0 ± 2.0
2+		775.3 ± 17.0	
3+		317.4 ± 42.6	

Average fission, capture cross sections, and uncertainties calculated with a constant flux from 600 eV to 40 keV are shown in Table 6. The calculations were done with the PUFF-IV code. The uncertainties in the average cross sections in the unresolved energy region are larger than the uncertainties in the resolved energy region. This is explained because the cross section in the resolved energy region is known much better. In addition, the resolved resonance formalism (Reich-Moore formalism), together with the Bayes' method, provides an accurate representation of the cross section and a better estimate of the RPCM and cross-section uncertainties. The methodology used in the unresolved resonance region is based on the Single-Level Breit-Wigner formalism and the fitting of the average cross sections, which results in larger errors in the average cross sections.

Table 6. Uncertainty in the average fission and capture cross section calculated with PUFF-IV in the unresolved energy region

E_{\min} (eV)	E_{\max} (eV)	σ_f (barns)	Relative standard deviation (%)	σ_γ (barns)	Relative standard deviation (%)
600.0	1000.0	12.476	3.7	2.435	7.7
1000.0	1500.0	9.223	4.0	1.792	8.2
1500.0	2000.0	7.959	4.0	1.537	8.0
2000.0	3000.0	6.676	4.1	1.293	7.8
3000.0	4000.0	5.836	4.1	1.075	7.8
4000.0	6000.0	4.907	4.5	0.887	7.8
6000.0	10000.0	4.146	5.2	0.638	7.9
10000.0	15000.0	3.561	6.4	0.535	8.2
15000.0	20000.0	3.203	7.8	0.477	8.1
20000.0	25000.0	2.971	9.0	0.451	8.0
25000.0	30000.0	2.816	8.0	0.423	8.8
30000.0	40000.0	2.672	9.0	0.383	8.8

4. PROCESSING OF THE ^{233}U COVARIANCE DATA

The resolved and unresolved resonance region covariance data generated with SAMMY were converted into the ENDF format specified for FILE 32. The ENDF covariance format for the

resolved resonance region allows two options: LCOMP = 1 for which the full covariance data and correlations are entered explicitly, and LCOMP = 2 (compact formalism) that was developed to alleviate the use of computer storage. The LCOMP = 1 option lead to a file of 100 MB. The ENDF unresolved resonance format is very restricted, permitting only representation of the average unresolved resonance parameter uncertainties and covariance for the entire energy region. This format was used because there is no other alternative to represent the unresolved resonance covariance in ENDF. For the energies above 40 keV to 20 MeV, the ENDF format given in FILE 33 was used.

The evaluated covariance data were added to the existing ^{233}U ENDF/B-VII cross-section evaluation²³ and processed with the computer codes PUFF-IV and ERRORJ. In the resolved resonance region, the uncertainty in the average cross section obtained with SAMMY, PUFF-IV, and ERRORJ are in good agreement. SAMMY and PUFF-IV uncertainties are identical. It appears that the slight difference found in the ERRORJ results could result from the different procedure used for performing derivatives in these codes. Derivatives in the ERRORJ code are done numerically, whereas in SAMMY and PUFF-IV they are performed analytically. In the unresolved and high-energy regions, PUFF-IV and ERRORJ calculated uncertainties are identical. Data averaged, including cross sections and the number of neutrons per fission, $\bar{\nu}$, (prompt and total) and their respective uncertainties were generated in the 44-neutron group structure of the SCALE system.²⁴ The results are displayed in Figs. 2–6. Figure 2 shows the average total $\bar{\nu}$ and the uncertainties. The prompt $\bar{\nu}$ and the uncertainties are shown in Fig. 3.

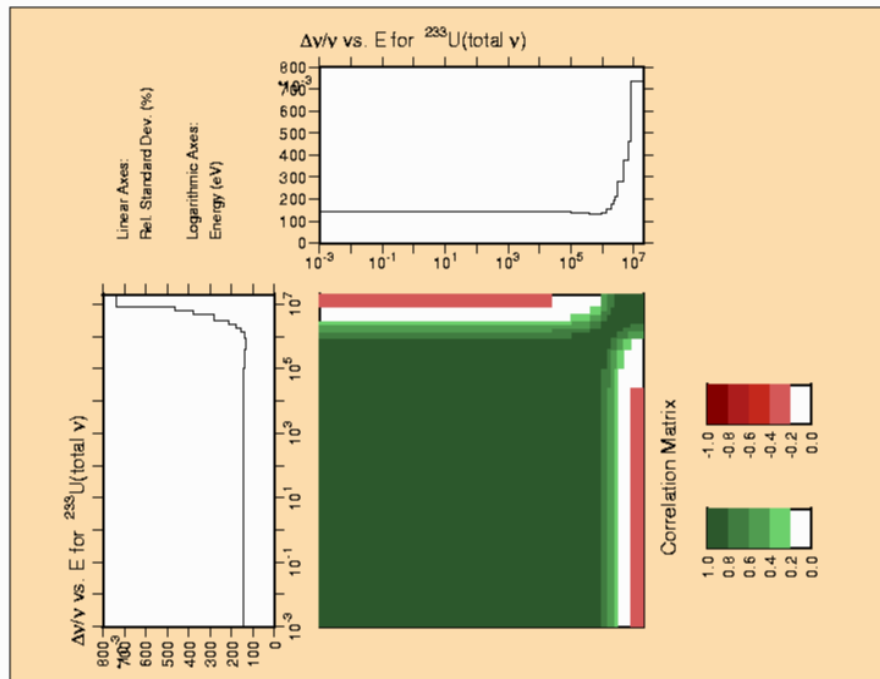


Fig. 2. Total $\bar{\nu}$ and uncertainties calculated in the 44-neutron groups of the SCALE system.

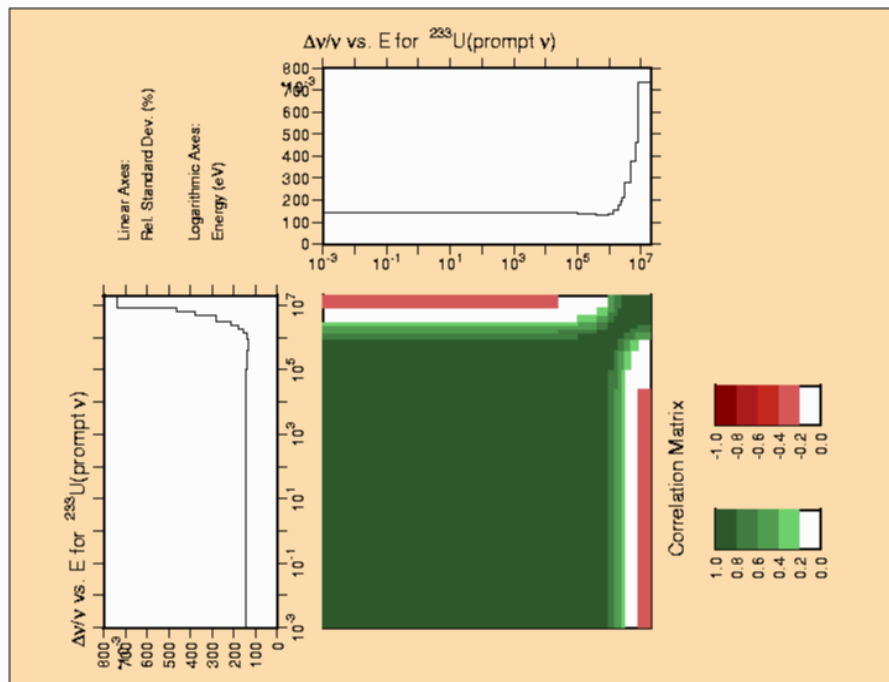


Fig. 3. Prompt $\bar{\nu}$ and uncertainties calculated in the 44-neutron groups of the SCALE system.

The 44-neutron group cross sections and uncertainties are shown in Figs. 4–6. The total cross sections are shown in Fig. 4. Uncertainties in the total cross sections range from 1 to 3.5%. Fission cross sections and uncertainties are displayed in Fig. 5. The maximum uncertainties in the fission cross sections in the resonance region (resolved and unresolved) are 4.5%. In the energy region above 40 keV to 20 MeV (high-energy region), the uncertainties in the fission cross sections can be as high as 9%. Capture cross section and uncertainties are shown in Fig. 6. As one would expect, high uncertainties in the capture cross sections are observed in the energy range above 40 keV. These results are consistent with the error in experimental data (systematic and statistical).

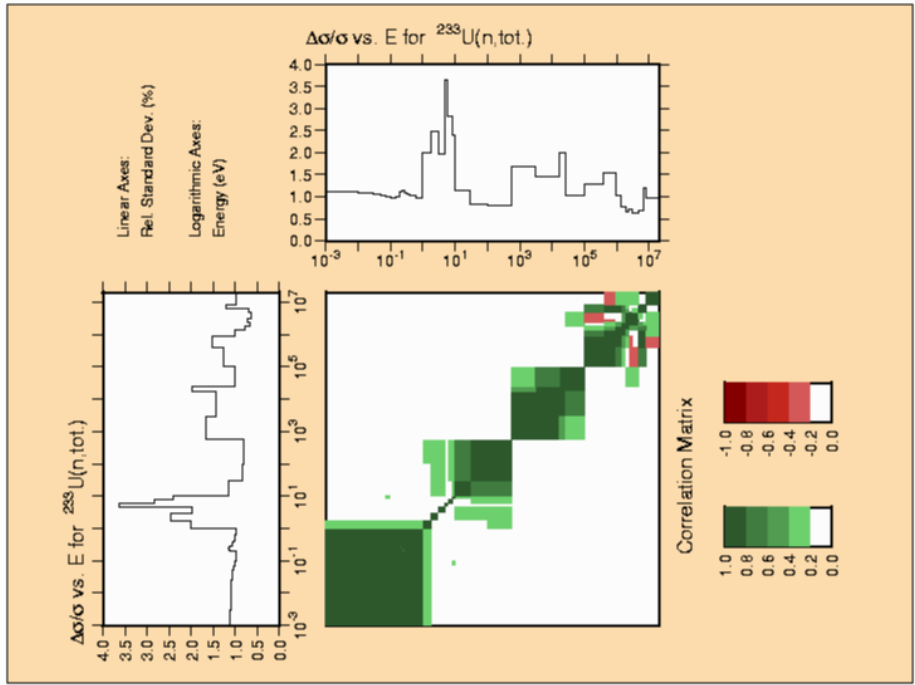


Fig. 4. ^{233}U total cross section calculated in the 44-neutron group structure of the SCALE system.

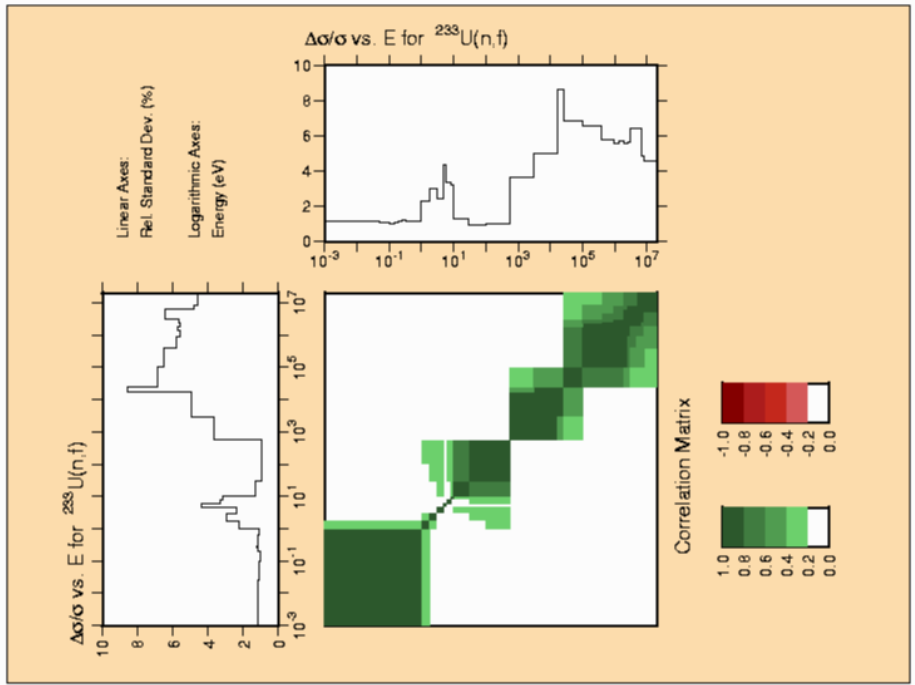


Fig. 5. ^{233}U fission cross section calculated in the 44-neutron group structure of the SCALE system.

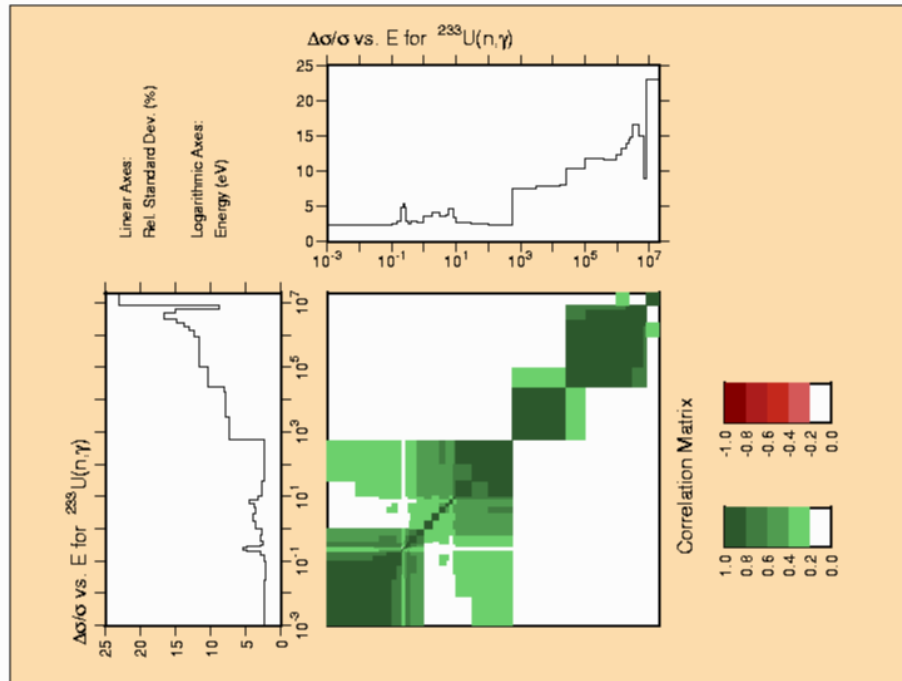


Fig. 6. ^{233}U capture cross section calculated in the 44-neutron group structure of the SCALE system.

5. PROCESSING OF ^{233}U ENDF FILE

The ^{233}U ENDF file was used to generate *centrm* formatted data and group-averaged cross section data along with the covariance information. The AMPX module *polident* was used to create point-wise cross section data at a temperature of $T = 0$ K. The energy mesh was generated to a precision of 0.001. The AMPX module *tgel* was used to calculate the total cross section as the sum of the relevant point-wise cross section data at $T = 0$ K. The AMPX module *broaden* was used to calculate the cross section data at temperatures $T = 0$ K, 300 K, 600 K, 900 K, 1200 K, and 2400 K. The resulting tab1 formatted file was converted to double precision using the module *charmin* so that the modules *bic* and *cajun* can be used to convert the data into a *centrm* formatted data file using the scale identifier 7009222.

The full AMPX input to generate the *centrm* library is

```
=shell
ln -fs /home/dw8/u233/U233.endf ft11f001
end
=polident
-1$$ 5000000
0$$ 30 e
1$$ 1 t
2$$ 9222 11 2 6 e
4** a5 0.001 e
6$$ a3 0 15000 t
end
```

```

=shell
cp ft30f001 /home/dw8/u233/polident/u233
cp ft32f001 /home/dw8/u233/polident/u233.ft32
end
=tgel
-1$$ 5000000
0$$ 30 31 e t
end
=broaden
limit=5000000
logpt=31 logdp=34
t= 0 300 600 900 1200 2400
end
=shell
cp ft34f001 /home/dw8/u233/broaden/u233
end
=charmin
limit=5000000
in=34 out=35 single to double end
end
=bic
limit=5000000
lsu input=35 output=36 version=6
title=u233      9222 92233 ENDFB V7 RELO REV0 MOD0 AMPX 06/29/05 n-ENDF-VIIb0.dat
end
=shell
cp ft36f001 /home/dw8/u233/centrmlib/u233
end
=shell
ln -fs /home/dw8/u233/centrmlib/u233 ft37f001
end
=cajun
-1$$ 5000000
0$$ 38
1$$ 1 e t
2$$ 37 1 t
3$$      9222
4$$ 7009222
5$$ 0
t
end
=shell
cp ft38f001 /home/dw8/u233/centrmlib/92233-0
end

```

The AMPX modules *pickeze* and *jergens* are used to generate a weighting spectrum for the calculation of the group-averaged cross section data. The weighting spectrum is based on the point-wise cross section data at 300 K. The module *jergens* creates the following weighting spectra:

1. a Maxwellian-1/E-fission spectrum, 1/E above 10 MeV, identifier 1, and
2. the above Maxwellian-1/E-fission spectrum, divided by the total cross section data, identifier 1099.

Use the AMPX module *y12* to produce point-wise kinematic data and the AMPX module *x10* to calculate multigroup constants for neutron interaction. It uses the standard 238-group structure with 90 thermal neutron groups and a neutron yield of 12.298. As a weighting function the Maxwellian-1/E-fission spectrum, 1/E above 10 MeV, normalized to the total cross section is

used. To calculate the cross section data in the unresolved resonance region, the AMPX module *prude* is used. The cross section data are generated for the background cross sections $\sigma_0 = 1.0 \times 10^{+8}$, $1.0 \times 10^{+6}$, $1.0 \times 10^{+5}$, and $1.0 \times 10^{+4}$ and temperatures of 1000 K, 100 K, 10 K, 1 K, and 1.0×10^{-6} K. These cross section data are converted to Bondarenko factors using the AMPX module *tabu*. Again the Maxwellian-1/E-fission spectrum, 1/E above 10 MeV, normalized to the total cross section is used as the weighting function. The AMPX module *unitab* is used to combine the group constants generated by *x10* and the Bondarenko factors generated by *tabu* into an AMPX master library. The thermal scattering matrix is calculated using the AMPX module *flange6* for temperatures 296 K, 600 K, 900 K, and 2000 K for the standard 238-group structure with 90 thermal neutron groups. The resulting master library is tested for validity using the AMPX module *rade*. The AMPX module *simonize* is used to assemble the AMPX master library containing all ^{233}U data.

The full AMPX input is

```
=shell
ln -fs /scratch/e5a/u233dir/thefinalu233covevaluation.dat ft11f001
ln -fs /home/dw8/u233/broaden/u233 ft29f001
end
=pickeze
-1$$ 5000000
0$$ 29 31
1$$ 1 0 0 1 0 e t
2$$ 9222
5** 300.
t
end
=jergens
-1$$ all 5000000 e
0$$ 31 30 18 1$$ 2 t
3$$ 1 0 4 t
3$$ 1099 4 0 t
2099 0 read 1.0 -1 0
2099 0 save 0 0 0
1099 2099 div 1.0 9222 1
1099 0 save 0 0 0
end
=y12
0$$ 32 11 e 1$$ 9222 2$$ 2 6 3$$ 32 8 8 8 5 t
t
end
=shell
cp ft32f001 /home/dw8/u233/fast.kinematics/u233
end
=x10
neutron
-1$$ 5000000
0$$ 1 30 31 32 1$$ 922233 238 90 0 5 0 0
2$$ 99 2099 9222 9222
3** 1.22989E+01
6$$ 99 2099
t
t
u233 9222 92233 ENDFB V7 REL0 REV0 MOD0 AMPX 08/04/05 n-ENDF-VIIb0.dat
end
=shell
cp ft01f001 /home/dw8/u233/238endf7.fast/u233
end
=prude
```

```

0$$ 34 1$$ 1 t
2$$ 9222 9 3 11 2 t
3** 1+8 1+6 1+5 1+4 1000 100 10 1 1-6
4** 300.0 900.0 2000.0 t
end
=tabu
-1$$ 500000 0$$ 2 34 30 1$$ 1 238 238 t
t Use the Standard Group Structure
u233 9222 92233 ENDFB V7 REL0 REV0 MOD0 AMPX 08/04/05 n-ENDF-VIIb0.dat
10$$ 9222 11$$ 99 3 2099 t
end
=shell
cp ft02f001 /home/dw8/u233/238endf7.BF/u233
cp ft34f001 /home/dw8/u233/unres.point/u233
end
=unitab
-1$$ 500000 0$$ 10 18 9 8 1 2 0 0 0 0 0 0 0 0 0
1$$ 1 2 6$$ 2000 500 t
2$$
92233 1 92233 1111
92233 2 9222 4444
t
end
=rade
-1$$ 5000000
1$$ 10 e t
end
=shell
cp ft10f001 /home/dw8/u233/238endf7.master/u233
end
=flange6
t=296 t=600 t=900 t=2000 nl=3
igm=238 neg=90 iftg=149 master=4
za=92233 awr= 2.31043E+02 free= 1.22989E+01
end
end
=rade
1$$ 4 e t
end
=shell
cp ft04f001 /home/dw8/u233/238endf7.thermal/u233
end
=shell
ln -fs /home/dw8/u233/238endf7.master/u233 ft20f001
ln -fs /home/dw8/u233/238endf7.thermal/u233 ft21f001
end
=simonize
identifier=92233 master=1
id45= 7009222 source=endf
neutron=20 id19=92233
2dn=21 id19=92233 mt= 0
end
=rade
-1$$ 5000000
1$$ 1 e t
end
=shell
cp ft01f001 /home/dw8/u233/238endf7.masterfinal/u233
end

```

The new evaluation is included into the scale cross section library.

The covariance data are generated using the 44-group structure instead of the 238. The AMPX library containing the cross section data for the 238-group structure is therefore collapsed to the 44-group structure using a light-water reactor flux. The collapse is done using the AMPX module *malocs*. The 238-group ENDF/B-V SCALE library contains the flux used as identifier `mat = 99` and `mt = 9088`. Because the resulting AMPX library uses the scale id 92233 and the amp module *puff_iv* needs the endf material number, the module *ajax* is used to change the identifier prior to running *puff_iv*. A flux of Maxwellian - 1/E-Fission Spectrum is used over the whole range of covariances matrices generated.

The AMPX input is as follows

```
=shell
ln -sf /projects/scale/scale5/data/scale.rev14.xn238 ft88f001
ln -sf /home/dw8/u233/scale.rev14.xn238_withendf7_u233 ft89f001
end
=malocs
0$$ 89 20
1$$ 238 44 0 0 -88 0
3$$ 99 9008 e
1t
4$$ 7r1 2 3 2r4 5 6 7 2r8 8r9 14r10 6r11 10r12 13
    7r14 11r15 12r16 30r17 16r18 2r19 6r20 3r21 6r22 14r23
    27r24 10r25 5r26 27 28 29 2r30 31 32 33 2r34 2r35 3r36
    2r37 38 39 40 41 42 3r43 9r44
2t
end
=ajax
0$$ 1 e
1$$ 1 t
2$$ 20 1 t
3$$
92233
4$$
9222 t
end
=shell
cp ft01f001 /home/dw8/u233/u233_puff_ampx
end
=shell
ln -fs /home/dw8/ampx/u233/U233.endf ft32f001
ln -fs /home/dw8/ampx/u233/u233_puff_ampx ft11f001
end
=jergens
0$$ 0 12 18
1$$ 1 t
3$$ 1099 0 4 t
=puff_iv
-1$$ 400000000 e
1$$ -1 0 0 11 32 9222 -12 -11 -12 1 2 2 a16 -1 e t
5## 59 1099 e t
coverx file for u233
end
=shell
cp ft01f001 /home/dw8/ampx/u233/coverx/u233
end
```

The new coverx file is incorporated into the scale covariance libraries.

6. BENCHMARK CALCULATIONS AND DATA UNCERTAINTY

The covariance data were verified through their use in 82 criticality safety benchmark experiments from the *International Handbook of Evaluated Criticality Safety Benchmark Experiments*.²⁵ Only experiments suitable for one-dimensional (1-D) modeling were selected for the verification. The TSUNAMI-1D sequence from SCALE 5.1 (Ref. 24) was used to generate k_{eff} sensitivities to each group-wise cross section data value used in the calculation of each benchmark. The calculations were performed using the SCALE 5.1 238-group ENDF/B-VI cross section data library, which was amended to include ENDF/B-VII data for ^{233}U (v6-238_u233) and the SCALE 5.1 recommended covariance data set for ENDF/B-VI, which was amended to include the ^{233}U covariance data described above. The results with the updated libraries were compared to baseline results for the same cases using the standard SCALE 5.1 238-group ENDF/B-VI library (v6-238) and the SCALE 5.1 recommended covariance data set for ENDF/B-VI.

The benchmark experiments are identified in Table 7, where some basic characteristics of the systems and the k_{eff} values with the two cross-section data libraries are shown. The uncertainties in the k_{eff} values for these systems are shown in Figs. 7–20. In these figures, results from two library sets are shown: (1) the standard 238-group ENDF/B-VI cross section library and 44groupv6rec covariance library (identified as v6-238 in the figures) and (2) the 238-group ENDF/B-VI cross section library with ENDF/B-VII data for ^{233}U and the 44group v6rec covariance library with ENDF/B-VII data for ^{233}U (identified as v6-238_u233 in the figures).

Figures 7 and 8 show the total uncertainty due to all covariance data. For fast systems, the total uncertainty is reduced from ~8% with ENDF/B-VI data to ~3% with ENDF/B-VII data. A small reduction in uncertainty is observed for intermediate energy systems, and values are nearly constant for thermal systems. Examining the uncertainty in k_{eff} generated by each process, much of the reduction in total uncertainty is due to ^{233}U fission uncertainties, as shown in Fig. 9. All other processes, shown in Figs. 10–20, show much smaller variations between the libraries. Some processes were not available in ENDF/B-VI, such as the covariance between ^{233}U fission and ^{233}U elastic, ^{233}U n,2n, and ^{233}U n,n', shown in Figs. 14, 19, and 20, respectively.

Table 7. Benchmark experiments selected for verification of the ^{233}U covariance data

Case Number	Identifier	Description	EALF (eV)	Benchmark k-eff	Benchmark k-eff Uncertainty	k-eff v6-238	k-eff v6-238_u233
1	umf001t00x	^{233}U Metal, Fast Spectrum	1.11E+06	1.0000	0.0010	0.99380	1.00082
2	umf002t01x	^{233}U Metal, Fast Spectrum	1.02E+06	1.0000	0.0010	0.99854	1.00004
3	umf002t02x	^{233}U Metal, Fast Spectrum	1.06E+06	1.0000	0.0011	0.99626	0.99928
4	umf003t01x	^{233}U Metal, Fast Spectrum	1.08E+06	1.0000	0.0010	0.99722	0.99995
5	umf003t02x	^{233}U Metal, Fast Spectrum	1.06E+06	1.0000	0.0010	0.99935	1.00023
6	umf004t01x	^{233}U Metal, Fast Spectrum	9.60E+05	1.0000	0.0007	1.00497	1.00784
7	umf004t02x	^{233}U Metal, Fast Spectrum	8.58E+05	1.0000	0.0008	1.00827	1.00949
8	umf005t01x	^{233}U Metal, Fast Spectrum	9.45E+05	1.0000	0.0030	0.99536	0.99849
9	umf005t02x	^{233}U Metal, Fast Spectrum	7.67E+05	1.0000	0.0030	0.99765	0.99896
10	umf006t00x	^{233}U Metal, Fast Spectrum	9.96E+05	1.0000	0.0014	1.00191	1.00127
11	usi001t01x	^{233}U Solution, Intermediate Spectrum	6.78E+00	1.0000	0.0083	0.98960	0.99102
12	usi001t02x	^{233}U Solution, Intermediate Spectrum	7.92E+00	1.0000	0.0085	0.98455	0.98589
13	usi001t03x	^{233}U Solution, Intermediate Spectrum	8.52E+00	1.0000	0.0066	0.98518	0.98649
14	usi001t04x	^{233}U Solution, Intermediate Spectrum	3.71E+00	1.0000	0.0061	0.99399	0.99560
15	usi001t05x	^{233}U Solution, Intermediate Spectrum	9.12E+00	1.0000	0.0082	0.98823	0.98954
16	usi001t06x	^{233}U Solution, Intermediate Spectrum	4.27E+00	1.0000	0.0061	0.98729	0.98888
17	usi001t07x	^{233}U Solution, Intermediate Spectrum	9.55E+00	1.0000	0.0059	0.98531	0.98665
18	usi001t08x	^{233}U Solution, Intermediate Spectrum	4.52E+00	1.0000	0.0056	0.98217	0.98380
19	usi001t09x	^{233}U Solution, Intermediate Spectrum	7.31E+00	1.0000	0.0068	0.98207	0.98346
20	usi001t10x	^{233}U Solution, Intermediate Spectrum	1.00E+01	1.0000	0.0053	0.98187	0.98327
21	usi001t11x	^{233}U Solution, Intermediate Spectrum	7.72E+00	1.0000	0.0057	0.98255	0.98400
22	usi001t12x	^{233}U Solution, Intermediate Spectrum	4.41E+00	1.0000	0.0091	0.98559	0.98750
23	usi001t13x	^{233}U Solution, Intermediate Spectrum	5.03E+00	1.0000	0.0071	0.98586	0.98768
24	usi001t14x	^{233}U Solution, Intermediate Spectrum	2.29E+00	1.0000	0.0052	0.99150	0.99355
25	usi001t15x	^{233}U Solution, Intermediate Spectrum	5.40E+00	1.0000	0.0075	0.98353	0.98532
26	usi001t16x	^{233}U Solution, Intermediate Spectrum	1.79E+00	1.0000	0.0028	0.97659	0.97879
27	usi001t17x	^{233}U Solution, Intermediate Spectrum	2.53E+00	1.0000	0.0055	0.98996	0.99198

Table 7. Benchmark experiments selected for verification of the ²³³U covariance data (continued)

Case Number	Identifier	Description	EALF (eV)	Benchmark k-eff	Benchmark k-eff Uncertainty	k-eff v6-238	k-eff v6-238_u233
28	usi001t18x	²³³ U Solution, Intermediate Spectrum	5.79E+00	1.0000	0.0057	0.98159	0.98338
29	usi001t19x	²³³ U Solution, Intermediate Spectrum	6.03E+00	1.0000	0.0083	0.97828	0.98010
30	usi001t20x	²³³ U Solution, Intermediate Spectrum	2.99E+00	1.0000	0.0056	0.98105	0.98308
31	usi001t21x	²³³ U Solution, Intermediate Spectrum	6.28E+00	1.0000	0.0050	0.97579	0.97766
32	usi001t22x	²³³ U Solution, Intermediate Spectrum	6.43E+00	1.0000	0.0049	0.98077	0.98270
33	usi001t23x	²³³ U Solution, Intermediate Spectrum	4.70E+00	1.0000	0.0047	0.99177	0.99373
34	usi001t24x	²³³ U Solution, Intermediate Spectrum	1.97E+00	1.0000	0.0081	0.99618	0.99891
35	usi001t25x	²³³ U Solution, Intermediate Spectrum	2.25E+00	1.0000	0.0081	0.98842	0.99106
36	usi001t26x	²³³ U Solution, Intermediate Spectrum	2.37E+00	1.0000	0.0065	0.99192	0.99452
37	usi001t27x	²³³ U Solution, Intermediate Spectrum	1.24E+00	1.0000	0.0051	0.99104	0.99375
38	usi001t28x	²³³ U Solution, Intermediate Spectrum	2.53E+00	1.0000	0.0061	0.98609	0.98866
39	usi001t29x	²³³ U Solution, Intermediate Spectrum	2.62E+00	1.0000	0.0098	0.97980	0.98237
40	usi001t30x	²³³ U Solution, Intermediate Spectrum	1.45E+00	1.0000	0.0053	0.97849	0.98117
41	usi001t31x	²³³ U Solution, Intermediate Spectrum	2.67E+00	1.0000	0.0071	0.99334	0.99594
42	usi001t32x	²³³ U Solution, Intermediate Spectrum	2.77E+00	1.0000	0.0053	0.97788	0.98051
43	usi001t33x	²³³ U Solution, Intermediate Spectrum	2.07E+00	1.0000	0.0046	0.99497	0.99760
44	ust001t01x	²³³ U Solution, Thermal Spectrum	3.90E-02	1.0000	0.0031	0.99867	1.00555
45	ust001t02x	²³³ U Solution, Thermal Spectrum	3.96E-02	1.0005	0.0033	0.99862	1.00550
46	ust001t03x	²³³ U Solution, Thermal Spectrum	4.02E-02	1.0006	0.0033	0.99812	1.00501
47	ust001t04x	²³³ U Solution, Thermal Spectrum	4.08E-02	0.9998	0.0033	0.99810	1.00499
48	ust001t05x	²³³ U Solution, Thermal Spectrum	4.14E-02	0.9999	0.0033	0.99740	1.00431
49	ust005t01x	²³³ U Solution, Thermal Spectrum	6.06E-02	1.0060	0.0020	1.00122	1.00684
50	ust008t01x	²³³ U Solution, Thermal Spectrum	3.68E-02	1.0006	0.0029	0.99722	1.00424
51	ust012t06x	²³³ U Solution, Thermal Spectrum	7.89E-02	0.9987	0.0011	1.00339	1.00861
52	ust015t01x	²³³ U Solution, Thermal Spectrum	1.09E+00	1.0000	0.0075	0.99372	0.99701
53	ust015t02x	²³³ U Solution, Thermal Spectrum	1.22E+00	1.0000	0.0070	0.98840	0.99159
54	ust015t03x	²³³ U Solution, Thermal Spectrum	1.29E+00	1.0000	0.0068	0.98912	0.99227
55	ust015t04x	²³³ U Solution, Thermal Spectrum	7.10E-01	1.0000	0.0041	0.98996	0.99313
56	ust015t05x	²³³ U Solution, Thermal Spectrum	1.35E+00	1.0000	0.0055	0.98848	0.99158

Table 7. Benchmark experiments selected for verification of the ²³³U covariance data (continued)

Case Number	Identifier	Description	EALF (eV)	Benchmark k-eff	Benchmark k-eff Uncertainty	k-eff v6-238	k-eff v6-238_u233
57	ust015t06x	²³³ U Solution, Thermal Spectrum	1.40E+00	1.0000	0.0099	0.97890	0.98199
58	ust015t07x	²³³ U Solution, Thermal Spectrum	7.81E-01	1.0000	0.0070	0.98754	0.99070
59	ust015t08x	²³³ U Solution, Thermal Spectrum	1.45E+00	1.0000	0.0067	0.97519	0.97824
60	ust015t09x	²³³ U Solution, Thermal Spectrum	1.48E+00	1.0000	0.0050	0.97050	0.97361
61	ust015t10x	²³³ U Solution, Thermal Spectrum	1.12E+00	1.0000	0.0051	0.99011	0.99322
62	ust015t11x	²³³ U Solution, Thermal Spectrum	6.83E-01	1.0000	0.0075	0.99664	1.00035
63	ust015t12x	²³³ U Solution, Thermal Spectrum	7.56E-01	1.0000	0.0069	0.99654	1.00017
64	ust015t13x	²³³ U Solution, Thermal Spectrum	7.96E-01	1.0000	0.0069	0.99420	0.99777
65	ust015t14x	²³³ U Solution, Thermal Spectrum	4.58E-01	1.0000	0.0036	0.99800	1.00155
66	ust015t15x	²³³ U Solution, Thermal Spectrum	8.35E-01	1.0000	0.0060	0.99171	0.99523
67	ust015t16x	²³³ U Solution, Thermal Spectrum	8.56E-01	1.0000	0.0043	0.99045	0.99395
68	ust015t17x	²³³ U Solution, Thermal Spectrum	4.95E-01	1.0000	0.0029	0.99735	1.00089
69	ust015t18x	²³³ U Solution, Thermal Spectrum	8.86E-01	1.0000	0.0056	0.97627	0.97974
70	ust015t19x	²³³ U Solution, Thermal Spectrum	9.00E-01	1.0000	0.0052	0.97642	0.97990
71	ust015t20x	²³³ U Solution, Thermal Spectrum	2.84E-01	1.0000	0.0079	0.99869	1.00318
72	ust015t21x	²³³ U Solution, Thermal Spectrum	3.11E-01	1.0000	0.0070	1.00064	1.00505
73	ust015t22x	²³³ U Solution, Thermal Spectrum	3.25E-01	1.0000	0.0062	0.99836	1.00270
74	ust015t23x	²³³ U Solution, Thermal Spectrum	3.38E-01	1.0000	0.0055	0.99598	1.00027
75	ust015t24x	²³³ U Solution, Thermal Spectrum	3.46E-01	1.0000	0.0051	0.99231	0.99656
76	ust015t25x	²³³ U Solution, Thermal Spectrum	2.20E-01	1.0000	0.0023	0.99705	1.00123
77	ust015t26x	²³³ U Solution, Thermal Spectrum	1.25E-01	1.0000	0.0066	0.99673	1.00196
78	ust015t27x	²³³ U Solution, Thermal Spectrum	1.29E-01	1.0000	0.0063	1.00068	1.00587
79	ust015t28x	²³³ U Solution, Thermal Spectrum	1.31E-01	1.0000	0.0058	0.99850	1.00364
80	ust015t29x	²³³ U Solution, Thermal Spectrum	1.33E-01	1.0000	0.0051	0.99682	1.00191
81	ust015t30x	²³³ U Solution, Thermal Spectrum	1.35E-01	1.0000	0.0048	0.99598	1.00103
82	ust015t31x	²³³ U Solution, Thermal Spectrum	1.36E-01	1.0000	0.0055	0.99506	1.00007

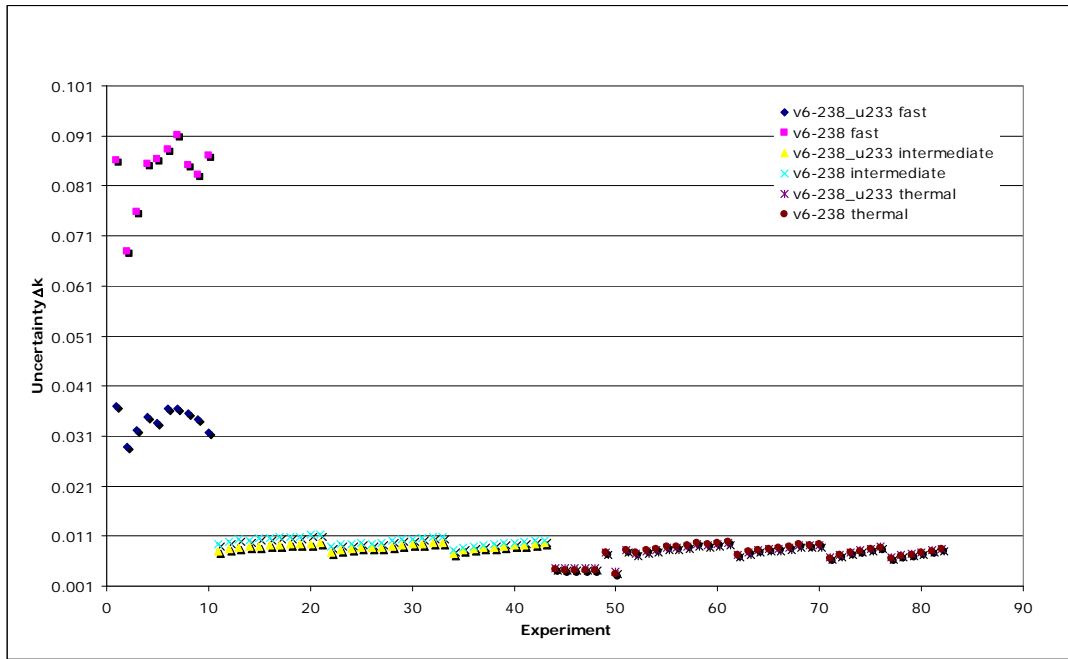


Fig. 7. Absolute k_{eff} uncertainties due to covariance data as a function of experiment number.

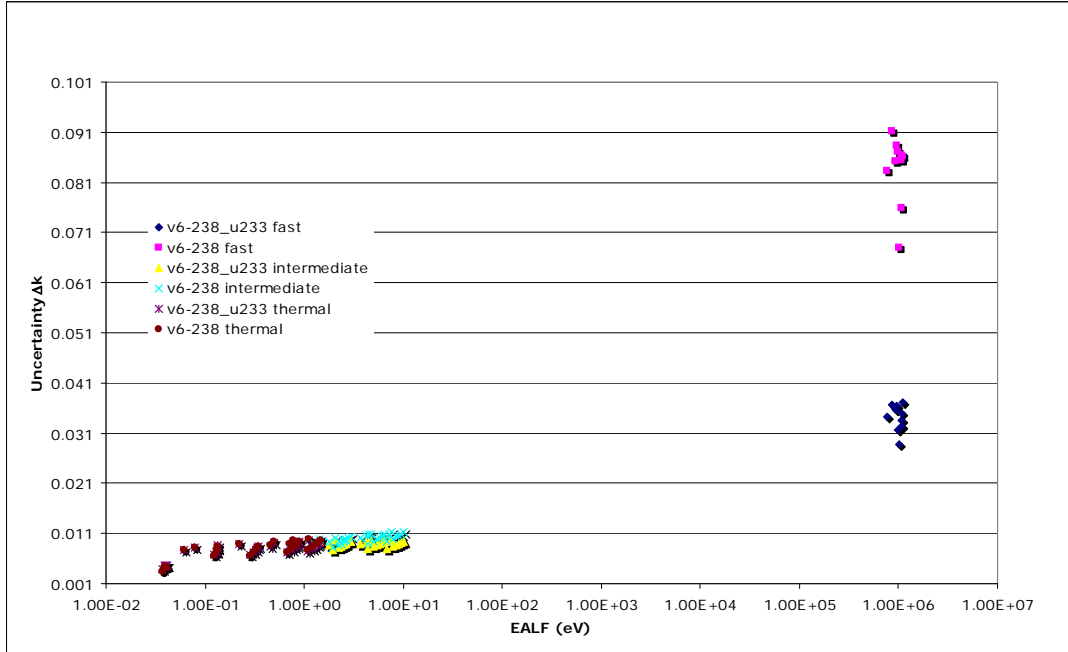


Fig. 8. Absolute k_{eff} uncertainties due to covariance data as a function of EALF.

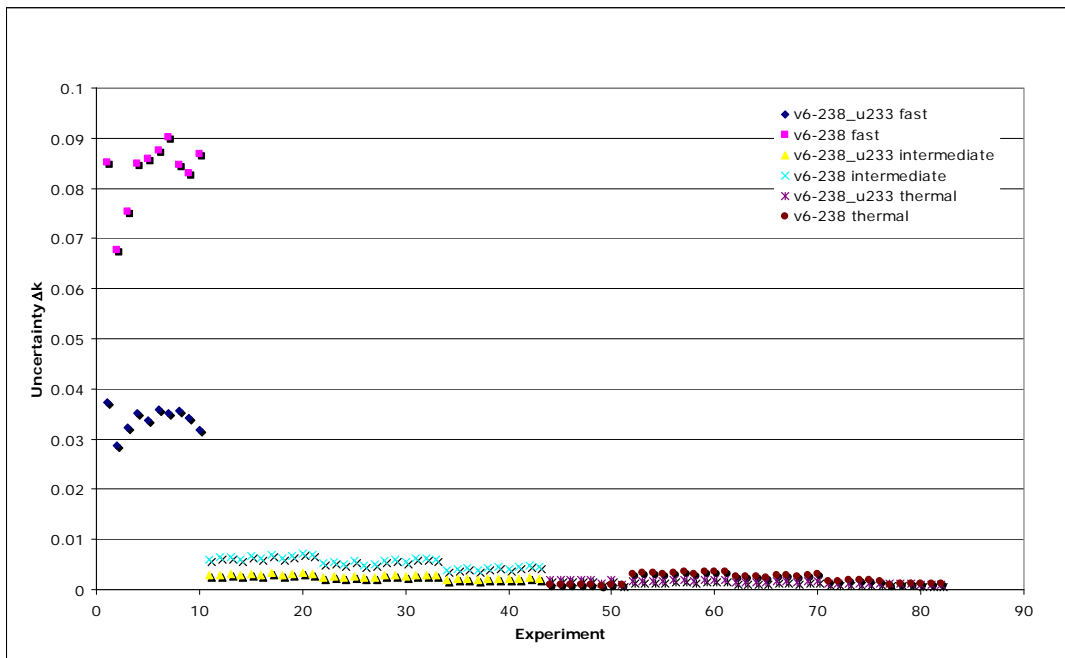


Fig. 9. Absolute k_{eff} uncertainties due to covariance data for ^{233}U fission.

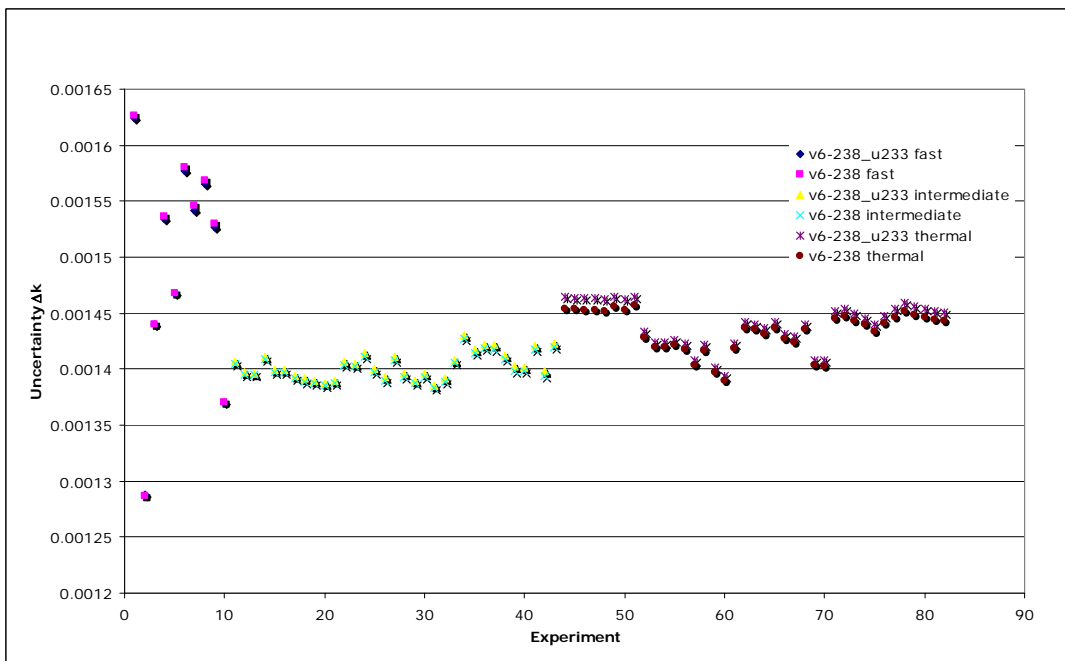


Fig. 10. Absolute k_{eff} uncertainties due to covariance data for ^{233}U $\bar{\nu}$.

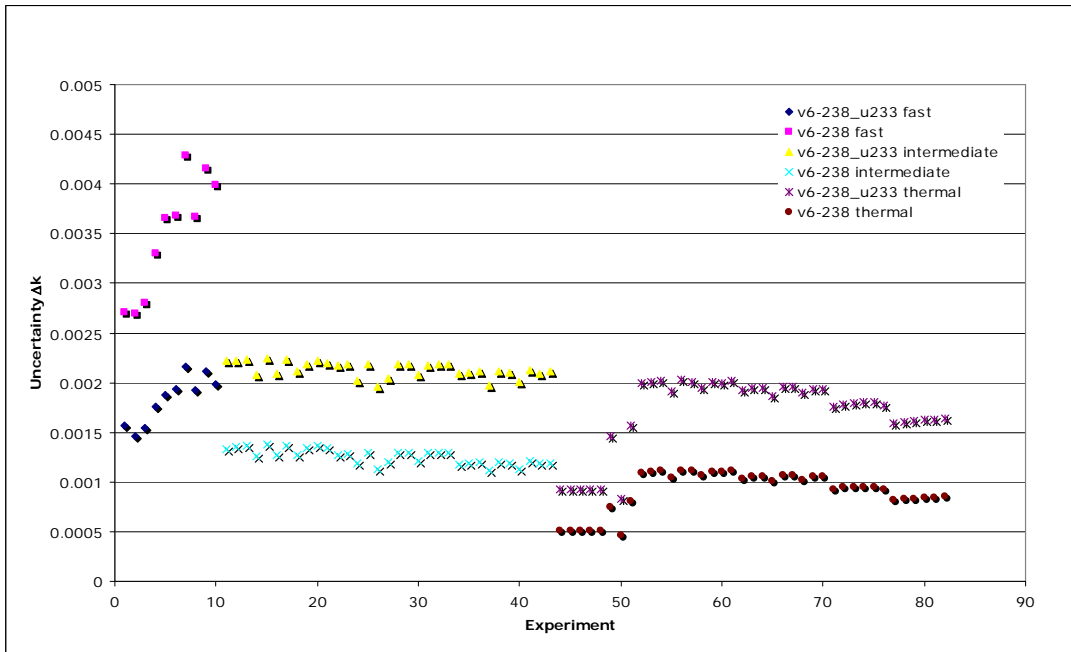


Fig. 11. Absolute k_{eff} uncertainties due to covariance data for ^{233}U n,gamma.

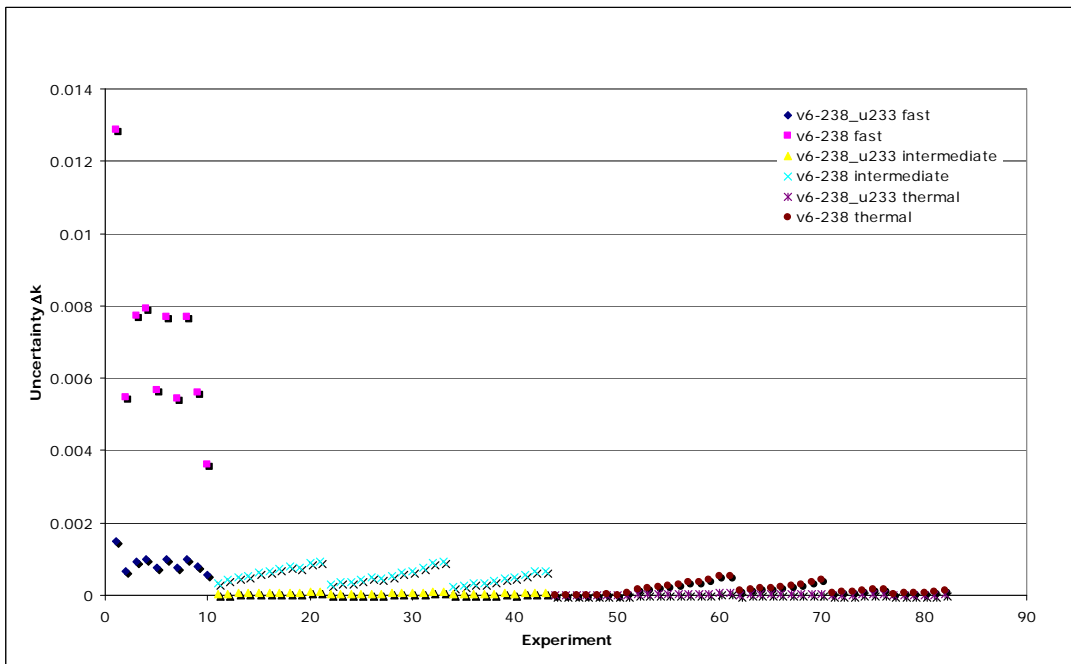


Fig. 12. Absolute k_{eff} uncertainties due to covariance data for ^{233}U elastic.

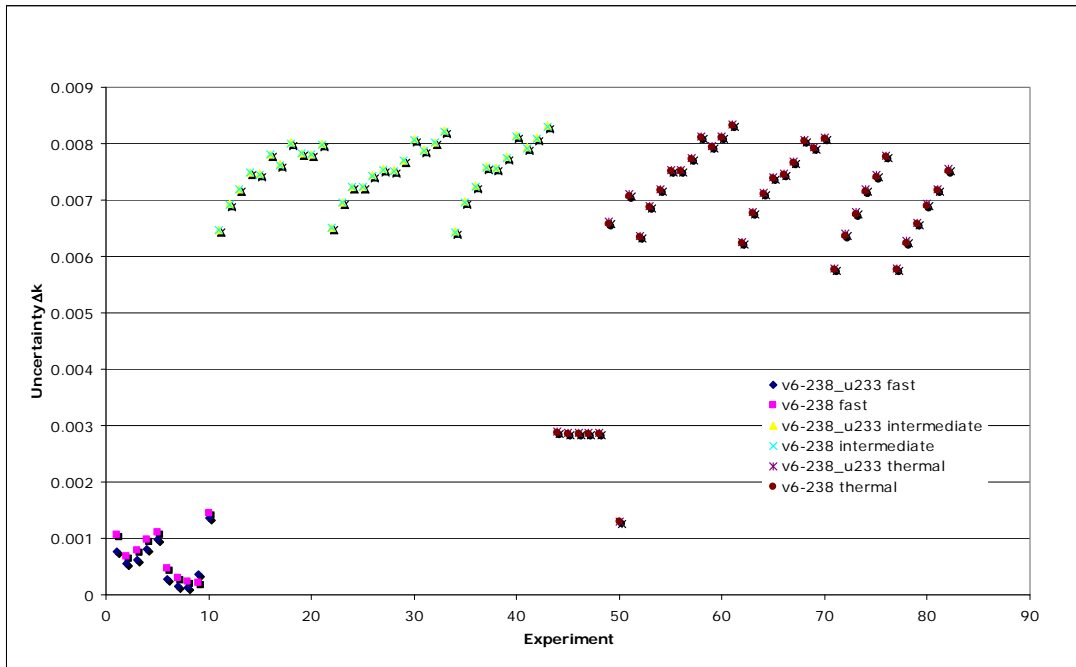


Fig. 13. Absolute k_{eff} uncertainties due to covariance data for ^{233}U chi.

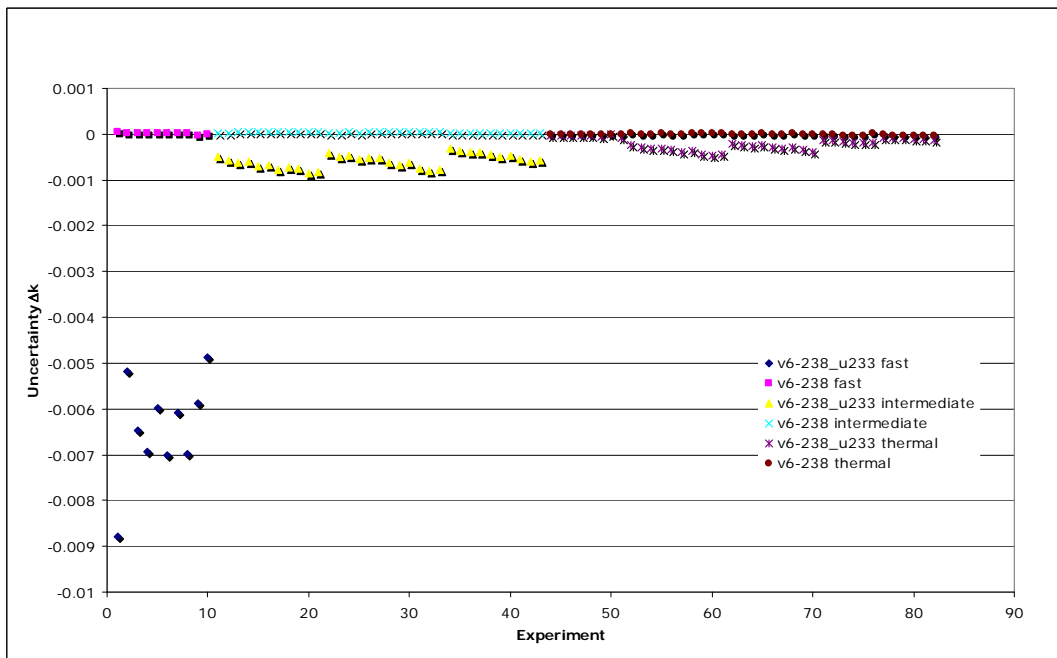


Fig. 14. Absolute k_{eff} uncertainties due to covariance data for ^{233}U fission to ^{233}U elastic.

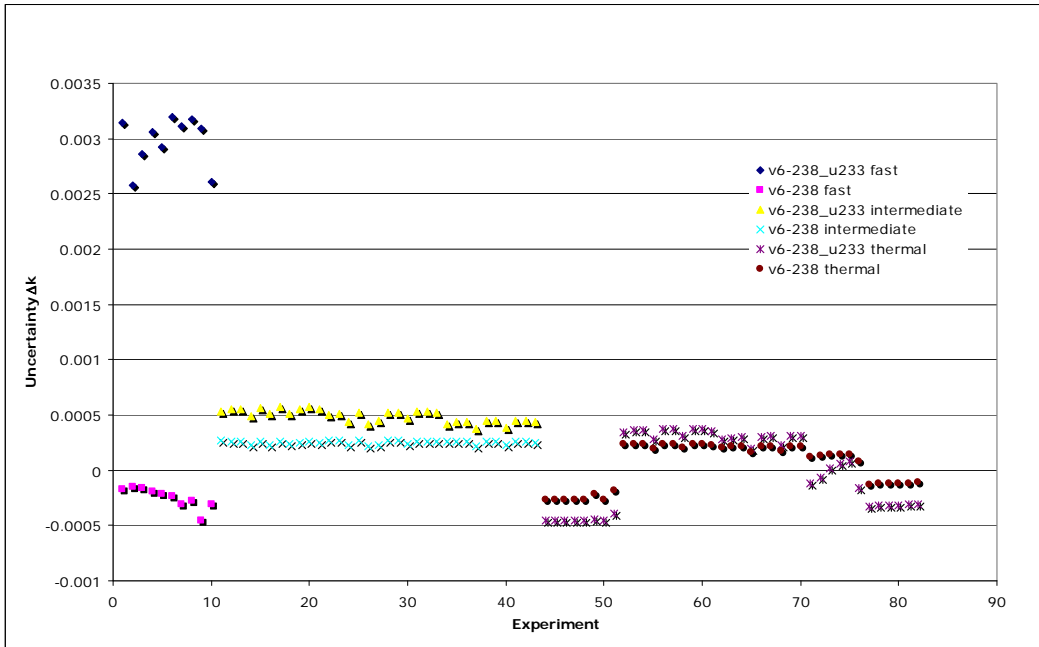


Fig. 15. Absolute k_{eff} uncertainties due to covariance data for ^{233}U fission to ^{233}U n,gamma.

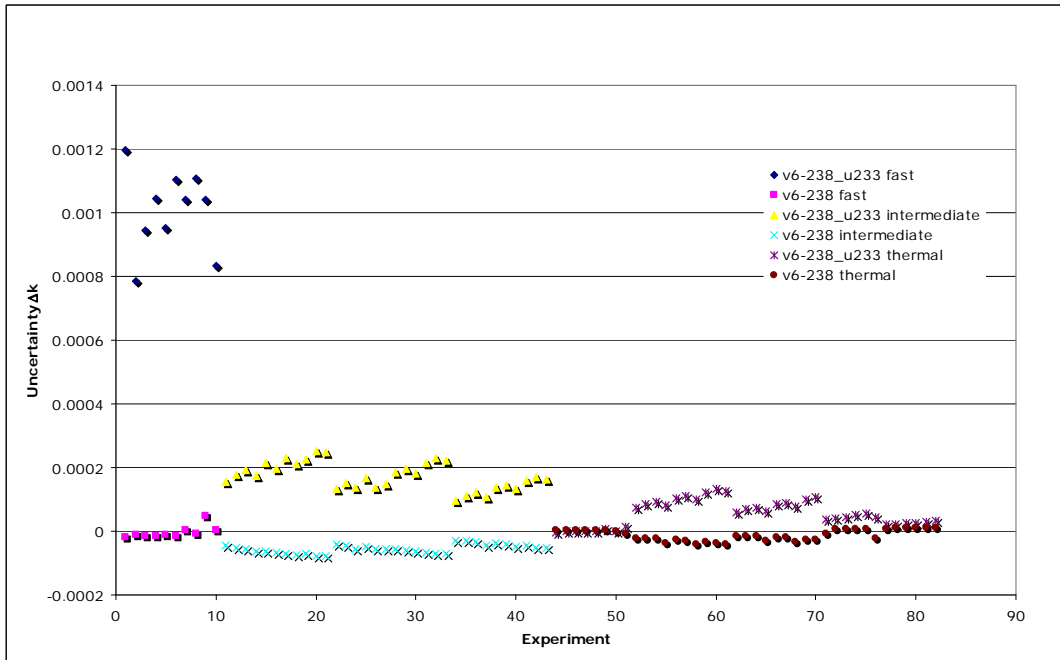


Fig. 16. Absolute k_{eff} uncertainties due to covariance data for ^{233}U n,gamma to ^{233}U elastic.

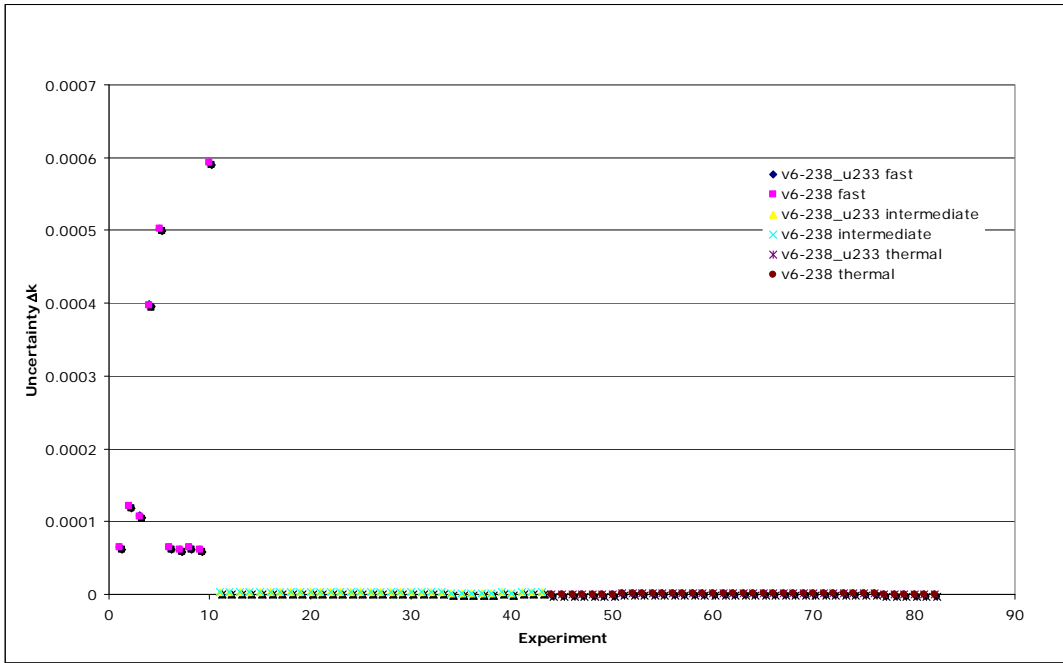


Fig. 17. Absolute k_{eff} uncertainties due to covariance data for ^{238}U fission to ^{233}U fission.

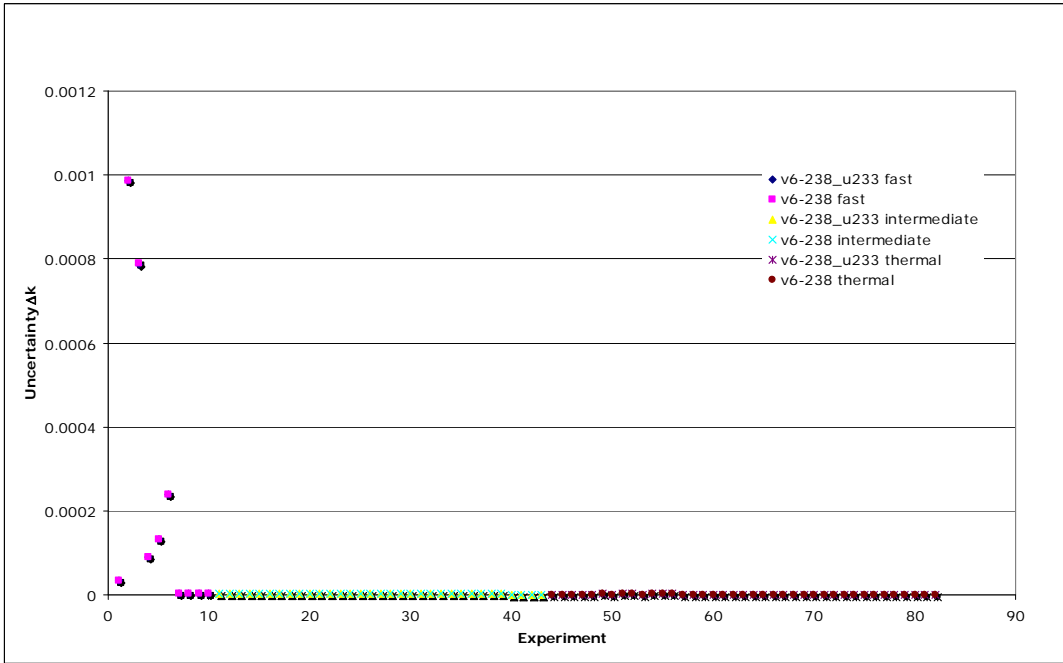


Fig. 18. Absolute k_{eff} uncertainties due to covariance data for ^{235}U fission to ^{233}U fission.

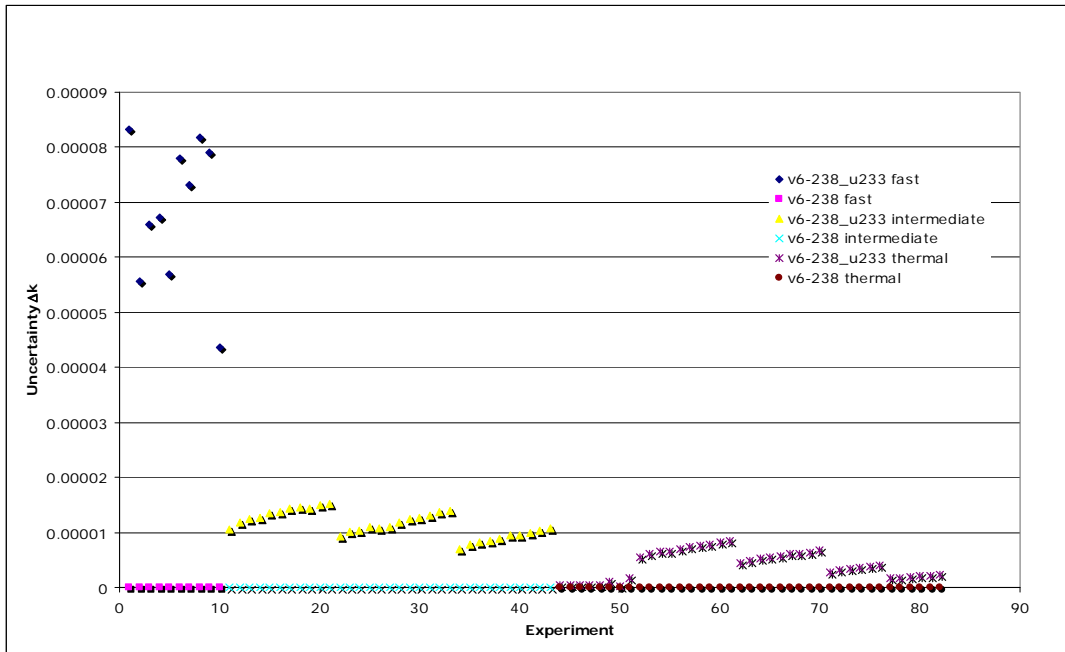


Fig. 19. Absolute k_{eff} uncertainties due to covariance data for ^{233}U n,2n.

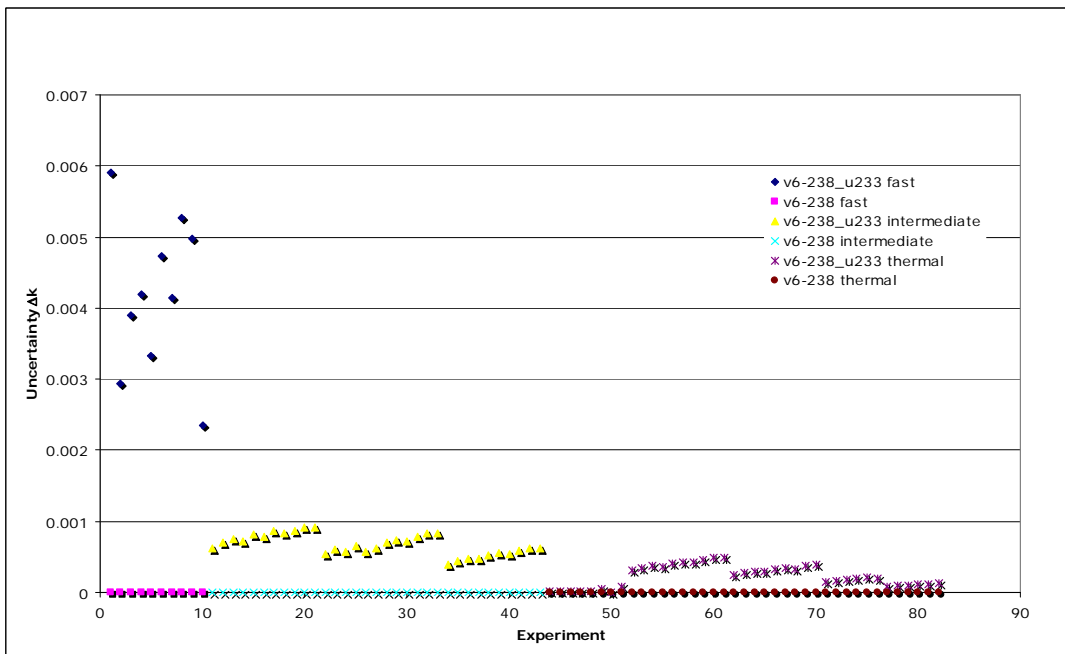


Fig. 20. Absolute k_{eff} uncertainties due to covariance data for ^{233}U n,n'.

7. CONCLUSIONS

Resonance-parameter covariance evaluations were performed in the resolved and unresolved resonance regions with the computer code SAMMY. The resolved resonance covariance evaluation was done in the energy range 0–600 eV, whereas the unresolved evaluation was performed in the energy region 600 eV to 40 keV. Above 40 keV to 20 MeV, the covariance data work was done at the IAEA. The covariance data were added to the ^{233}U ENDF/B/VII.0 evaluation and processed with the AMPX and PUFF-IV codes. Sensitivity analysis of 82 benchmark experiments with ^{233}U were done with the TSUNAMI code. The majority of the benchmark experiments used to verify the ^{233}U covariance data were taken from the *International Handbook of Evaluated Criticality Safety Benchmark Experiments*. For the fast systems the total uncertainty of the system multiplication factors was reduced from ~8% with ENDF/B-VI uncertainty to ~3% using the covariance evaluation done in this work. Small decreases in the uncertainty for thermal and intermediate energy systems are also observed. It appears that the reduction in the multiplication factor uncertainty is due to a decrease in the ^{233}U fission cross sections uncertainty. This is the result of a better resonance analysis and better differential fission cross section experiments used in the evaluation. The work presented here will support criticality safety calculations for the Oak Ridge National Laboratory Building 3019.

8. REFERENCES

1. N. M. Larson, *Updated Users' Guide for SAMMY: Multilevel R-Matrix Fits to Neutron Data Using Bayes' Equations*, ORNL/TM-9179/R7, Oak Ridge National Laboratory (2007).
2. L. C. Leal, H. Derrien, J. A. Harvey, K. H. Guber, N. M. Larson, and R. R. Spencer, *R-Matrix Resonance Analysis and Statistical Properties of the Resonance Parameters of ^{233}U in the Neutron Energy Range from Thermal to 600 eV*, ORNL/TM-2000/372, Oak Ridge National Laboratory and ENDF-365 (March 2001).
3. L. C. Leal, H. Derrien, N. M. Larson, and A. Courcelle, "An Unresolved Resonance Evaluation for ^{233}U from 600 eV to 40 keV," *2005 ANS Annual Meeting "The Next 50 Years: Creating Opportunities*, June 5–9, 2005, San Diego, California. *Trans. Am. Nucl. Soc.*, **92**, 665–666 (June 2005).
4. R. Capote, M. Sin, A. Trkov, et al., "Extension of the Nuclear Reaction Model Code EMPIRE to Actinides' Nuclear Data Evaluation," *Nuclear Data Conference*, Nice, France, April 22–27, 2007.
5. M. Herman, R. Capote, B. Carlson, P. Oblozinsky, M. Sin, A. Trkov, and V. Zerkin, "EMPIRE, nuclear reaction model code, version 2.19 (Lodi)," www.nndc.bnl.gov/empire219, March 2005.
6. D. L. Smith, *Covariance Matrices for Nuclear Cross Sections Derived from Nuclear Model Calculations*, ANL/NDM-159, Argonne National Laboratory, November 2004.
7. D. W. Muir, A. Trkov, I. Kodeli, et al., "The Global Assessment of Nuclear Data, GANDR," *Nuclear Data Conference*, Nice, France, April 22–27, 2007.
8. K. Raskach, Oak Ridge National Laboratory, personal communication (March 2006).
9. D. Wiarda and M. E. Dunn, *PUFF-IV: A Code for Processing ENDF Uncertainty Data into Multigroup Covariance Matrices*, ORNL/TM-2006/147, Oak Ridge National Laboratory (October 2006).
10. K. Kosako and N. Yanano, "Preparation of a Covariance Processing System for the Evaluated Nuclear Data File, JENDL," JNC TJ 9440 99-003, 1999 [in Japanese]; K. Kosako, "Covariance Data Processing Code: ERRORJ," in *Proceedings of the Specialists' Meeting of Reactor Group Constants, February 22–23, 2001*, JAERI-Conf 2001-009, ed. J. Katakura, JAERI, Tokai, Japan (2001).
11. *ENDF-102, Data Formats and Procedures for the Evaluated Nuclear Data File, ENDF-6*, written by Members of the Cross Section Evaluation Working Group, ed. V. McLane, C. L. Dunford, and P. F. Rose, BNL-NCS-4495, Brookhaven National Laboratory (April 2001). Updated BNL-NCS-449504-Rev, ed. M. Herman (June 2005).
12. L. C. Leal, G. Arbanas, H. Derrien, N. M. Larson, and B. Rearden, "Covariance Generation for ^{233}U in the Resolved Resonance Region for Criticality Safety Applications," *Mathematics and Computation, Supercomputing, Reactor Physics and Nuclear and Biological Applications*, Palais des Papes, Avignon, France, September 12–15, 2005.
13. K. H. Guber, R. R. Spencer, L. C. Leal, P. E. Koehler, J. A. Harvey, R. O. Sayer, H. Derrien, T. E. Valentine, D. E. Pierce, V. M. Cauley, and T. A. Lewis, "High-Resolution Transmission Measurements of U-233 Using a Cooled Sample At the Temperature T=11 K," *Nucl. Sci. Eng.*, **139(2)**, 111–117 (2001).

14. K. H. Guber, R. R. Spencer, L. C. Leal, J. A. Harvey, N. W. Hill, G. Dos Santos, R. O. Sayer, and D. C. Larson, "New High-Resolution Fission Cross-Section Measurements of U-233 in the 0.4-eV to 700-keV Energy Range," *Nuc. Sci. Eng.* **135(2)**, 141-149 (2000).
15. J. A. Harvey, C. L. Moore, and N. W. Hill, *Proc. Int. Conf. on Neutron Cross Section for Technology, Knoxville, Oct. 22–26, 1979*, NBS Special Publication 594, p. 690 (1980).
16. M. S. Moore, M. G. Miller, and O. D. Simpson, "Slow Neutron Total and Fission Cross Sections of U-233," *Phys. Rev.*, **118**, 714 (1960).
17. N. J. Pattenden and J. A. Harvey, "Measurement of the Neutron Total Cross Section of U²³³ from 0.07 to 10,000 ev," *Nuc. Sci. Eng.*, **17**, 404-410 (1963).
18. L. W. Weston, R. Gwin, G. De Saussure, R. W. Ingle, J. H. Todd, C. W. Craven, R. W. Hockenbury, and R. C. Block, "Neutron Fission and Capture Cross-Section Measurements for Uranium-233 in Energy Region 0.02 to 1 eV," *Nuc. Sci. Eng.* **42(2)**, 143 (1970).
19. J. Blons, "High-Resolution Measurements of Neutron-Induced Fission Cross-Sections for U-233, U-235, Pu-239 and Pu-241 Below 30 keV," *Nucl. Sci. Eng.*, **51(2)**, 130–147 (1973).
20. A. J. Deruytter and C. Wagemans, "Measurement and Normalization of Relative Uranium-233 Fission Cross-Section In Low Resonance Region," *Nucl. Sci. Eng.*, **54(4)**, 423–431 (1974).
21. H. Derrien, J. A. Harvey, K. H. Guber, L. C. Leal, and N. M. Larson, *Average Neutron Total Cross Sections in the Unresolved Energy Region from ORELA High Resolution Transmission Measurements*, ORNL/TM-2003/291 (2004).
22. J. C. Hopkins and B. C. Diven, "Neutron Capture To Fission Ratios In U²³³, U²³⁵, Pu²³³," *Nucl. Sci. Eng.*, **12**, 169–177 (1962).
23. M. B. Chadwick et al., "ENDF/B-VII.0: Next Generation Evaluated Nuclear Data Library for Nuclear Science and Technology," *Nuclear Data Sheet*, Vol. 107, December 2006.
24. *SCALE: A Modular Code System for Performing Standardized Computer Analyses for Licensing Evaluation*, ORNL/TM-2005/39, Version 5.1, Vols. I–III, "TSUNAMI-3D: Control Module for Three-Dimensional Cross-Section Sensitivity and Uncertainty Analysis for Criticality," Vol. I, Sect. C9, Oak Ridge National Laboratory (November 2006).
25. *International Handbook of Evaluated Criticality Safety Benchmark Experiments*, NEA/NSC/DOC(95)03, NEA Nuclear Science Committee, September 2006.

INTERNAL DISTRIBUTION

- | | |
|--------------------|------------------------------|
| 1. S. M. Bowman | 14. C. V. Parks |
| 2. B. L. Broadhead | 15. J. E. Rushton |
| 3. M. D. DeHart | 16. J. C. Wagner |
| 4. H. Derrien | 17. R. M. Westfall |
| 5. M. E. Dunn | 18. D. A. Wiarda |
| 6. I. C. Gauld | 19. M. L. Williams |
| 7. J. C. Gehin | 20. Central Research Library |
| 8. C. M. Hopper | 21. OTIC—RC, OSTI, CR |
| 9. J. O. Johnson | |
| 10. B. L. Kirk | |
| 11. N. M. Larson | |
| 12. L. C. Leal | |
| 13. D. E. Mueller | |

EXTERNAL DISTRIBUTION

22. J. Blair Briggs, Idaho National Laboratory, 2525 N. Fremont, P.O. Box 1625, Idaho Falls, ID 83415-3860
23. D. E. Carlson, U.S. Nuclear Regulatory Commission, RES/DSARE/REAHFB, MS T10-F13A, Washington, DC 20555-0001
24. J. M. Conde López, Consejo de Seguridad Nuclear, Jefe de Area de Ingeniería Nuclear, Subdirección General de Tecnología Nuclear, Justo Dorado, 11, 28040 Madrid, SPAIN
25. P. Cousinou, Institut de Protection et de Sûreté Nucleaire, Département de Recherches en Sécurité, CECI B.P. 6 - 92265 Fontenzy-Aux-Roses, Cedex, France
26. D. Erickson, Fluor Government Group, P.O. Box 1050, MSIN T5-54, Richland, WA 99352
27. A. Garcia, U.S. Department of Energy, Idaho Operations Office, Idaho Falls, ID 83401-1226
28. J. N. Gulliford, BNFL, R101, Rutherford House, Risley, Warrington, Cheshire WA3 6AS
29. D. Hayes, Los Alamos National Laboratory, P.O. Box 1663, MS J562, Los Alamos, New Mexico 87545
30. D. Heinrichs, Lawrence Livermore National Laboratory, MS L-128, 7000 East Ave., Livermore, CA 94550-9234
31. R. Y. Lee, U.S. Nuclear Regulatory Commission, RES/DSARE/SMSAB, MS T10-K8, Washington, DC 20555-0001
32. R. Little, Los Alamos National Laboratory, P.O. Box 1663, Los Alamos, New Mexico 87545
33. J. McKamy, U.S. Department of Energy, National Security Administration, NA-171, 19901 Germantown Road, Germantown, MD 20874
34. R. McKnight, Argonne National Laboratory, 9700 S. Cass Ave., Argonne, IL 60439
35. J. Morman, Argonne National Laboratory, 9700 S. Cass Ave., Argonne, IL 60439
36. J. C. Neuber, AREVA NP GmbH Mechanical Analyses NEEA-G, Kaiserleistrasse 29, 63005 Offenbach am Main Germany

37. P. Oblozinsky, Brookhaven National Laboratory, National Nuclear Data Center, Bldg. 197D, P.O. Box 5000, Upton, NY 11973-5000
38. H. Okuno, Japan Atomic Energy Research Institute, Department of Fuel Cycle, Safety Research, 2-4 Shirakata-Shirane, 319-1195 Tokai-mura, Naka-Gun, Ibaraki-ken, JAPAN
39. E. Sartori, OECD/NEA Data Bank, Le Seine-Saint Germain, 12 Boulevard des Iles, F-92130 Issy-les-Moulineaux, FRANCE
40. D. E. Dei, Naval Reactors, 1240 Isaac Hull Avenue SE, Stop 8011, Washington Navy Yard, D.C. 20376-8011
41. Dae Y. Chung, U.S. Department of Energy, EM-60, 0B050, 1000 Independence Ave., SW, Washington, D.C. 20585
42. R. E. Wilson, U.S. Department of Energy, Rocky Flats Project Office, Federal Building 55, P.O. Box 25547, Denver, CO 80025-0547